Exploring electrophilic hydrophosphination via metal phosphenium intermediates

Roman G. Belli, Vanessa Muir, Nicholas B. Dyck, Dimitrios A. Pantazis, Tânia P. A. Sousa, Carly R. Slusar, Hayley C. Parkin, and Lisa Rosenberg

2024

Chemistry–A European Journal
Research Article
doi.org/10.1002/chem.202302924
Chemistry Europe
European Chemical Societies Publishing
www.chemeurj.org

Exploring Electrophilic Hydrophosphination via Metal Phosphenium Intermediates

Roman G. Belli,[a] Vanessa Muir+,[a] Nicholas B. Dyck+,[a] Dimitrios A. Pantazis,[b] Tânia P. A. Sousa,[b] Carly R. Slusar,[a] Hayley C. Parkin,[a] and Lisa Rosenberg*[a]

Dedicated to Prof. Dr. Dietrich Gudat on the occasion of his retirement.

Two Mo(0) phosphenium complexes containing ancillary secondary phosphine ligands have been investigated with respect to their ability to participate in electrophilic addition at unsaturated substrates and subsequent P–H hydride transfer to "quench" the resulting carbocations. These studies provide stoichiometric "proof of concept" for a proposed new metal-catalyzed electrophilic hydrophosphination mechanism. The more strongly Lewis acidic phosphenium complex, $[Mo(CO)_4(PR_2H)(PR_2)]^+$ (R = Ph, Tol^p), cleanly hydrophosphinates 1,1-diphenylethylene, benzophenone, and ethylene, while other substrates react rapidly to give products resulting from competing electrophilic processes. A less Lewis acidic complex, $[Mo(CO)_3(PR_2H)_2(PR_2)]^+$, generally reacts more slowly but participates in clean hydrophosphination of a wider range of unsaturated substrates, including styrene, indene, 1-hexene, and cyclohexanone, in addition to 1,1-diphenylethylene, benzophenone, and ethylene. Mechanistic studies are described, including stoichiometric control reactions and computational and kinetic analyses, which probe whether the observed P–H addition actually does occur by the proposed electrophilic mechanism, and whether hydridic P–H transfer in this system is intra- or intermolecular. Preliminary reactivity studies indicate challenges that must be addressed to exploit these promising results in catalysis.

Introduction

Metal-catalyzed hydrophosphination has received increasing attention as an atom-economic route to the preparation of new organophosphines.[1] A major challenge in this field is that the unsaturated substrate scope is generally limited to electron-deficient alkenes or alkynes.[1c,l] This arises from the fact that most examples of metal-catalyzed hydrophosphination rely on the intermediacy of metal phosphido complexes, containing formally anionic PR_2^- ligands.[1g,p] These M-PR_2 functionalities are excellent nucleophiles (Figure 1a),[2] which allows them to participate in P–C bond formation either through migratory insertion of the unsaturated substrate into the M–P bond (most often reported for d^0 metal complexes) or by conjugate addition of the phosphido ligand to the unsaturated substrate (observed for a wide range of complexes but most particularly for late metals) (Scheme 1). The "outer-sphere", conjugate addition mechanism is likely to occur primarily for activated, electron-deficient substrates, especially acrylates or α,β-unsaturated nitriles. And, although classic organometallic mechanistic concepts might lead us to expect that all alkenes can participate in "inner-sphere", M-PR_2 insertion chemistry,[3] in

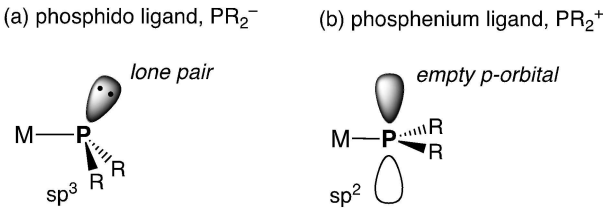

Figure 1. Two classes of M-PR_2 ligand with opposite M–P polarization (formal charges not shown). (a) The lone pair at P renders metal phosphido complexes P-nucleophilic. (b) The empty *p*-orbital at P (and localized positive charge) renders metal phosphenium complexes electrophilic.[5,6]

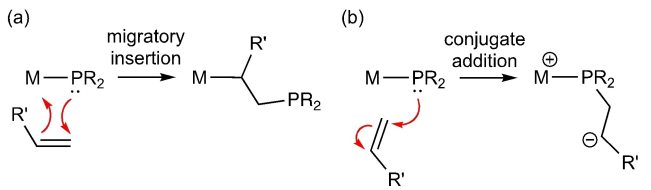

Scheme 1. a) Inner- and b) outer-sphere P–C bond-forming steps in catalytic hydrophosphination that rely on nucleophilicity of metal phosphido intermediates.

[a] Dr. R. G. Belli, V. Muir,+ N. B. Dyck,+ C. R. Slusar, H. C. Parkin, Prof. L. Rosenberg
Department of Chemistry, University of Victoria, P.O. Box 1700, STN CSC, Victoria, British Columbia, Canada V8W 2Y2
E-mail: lisarose@uvic.ca
[b] Dr. D. A. Pantazis, T. P. A. Sousa
Max-Planck-Institut für Kohlenforschung, Kaiser-Wilhelm-Platz 1, 45470 Mülheim an der Ruhr, Germany
[+] These authors contributed equally.

Supporting information for this article is available on the WWW under https://doi.org/10.1002/chem.202302924

practice there are remarkably few examples of simple (electron-rich) alkene substrates for metal-catalyzed hydrophosphination.[4]

We are interested in exploring new mechanistic paradigms for hydrophosphination that will allow a much broader range of substrates to be employed. While expanding the range of phosphine substrates is also a goal (most studies employ just PPh_2H), in this study we have focused on the potential to target a wider variety of unsaturated substrates, including simple, unactivated alkenes, through the design of a system relying on intermediates containing cationic phosphenium ligands (PR_2^+, Figure 1b). For example, Scheme 2 shows a possible catalytic cycle involving a metal phosphenium complex that electronically inverts the fundamental steps we have previously established for the outer-sphere hydrophosphination of activated alkenes catalyzed by half-sandwich Ru phosphido complexes.[7] The cycle relies on electrophilic addition of the phosphenium ligand to the unsaturated substrates (instead of nucleophilic addition of a phosphido ligand), and the ability of a coordinated secondary phosphine to act as a hydride transfer agent (instead of acting as a proton transfer reagent).

As isoelectronic analogues of the Fischer carbene, phosphenium ligands have been most closely examined in their capacity as tunable ancillary ligands, typically with stabilizing heteroatom (NR_2, OR) substituents.[8] However, the electrophilic reactivity of metal phosphenium complexes, required for step A in the proposed cycle, is well established,[5,9] and has been exploited in stoichiometric P–C bond forming reactions involving electrophilic substitution.[10] This reactivity has not yet been harnessed in catalytic (hydro)phosphination.[11]

We and others have also shown that metal phosphenium complexes can be prepared by electrophilic abstraction of the P–H bonds in coordinated secondary phosphines,[9b,12, 13] as required for the carbocation "quenching" shown in step B in Scheme 2. This is a departure from traditional P–X abstraction routes to metal-coordinated phosphenium, where X = halide, alkoxide, or amide.[8] Seminal work demonstrating the desired $P^{\delta+}$–$H^{\delta-}$ bond polarization in secondary phosphines comes from the chemistry of diazaphospholenes.[14] These "N-heterocyclic" secondary phosphines are hydride donors and participate in the stoichiometric hydrophosphination of a variety of unsaturated substrates, including aldehydes, ketones, and CO_2.[14,15] The regiochemistry of P–H addition to C=O results from the delivery of PR_2^+ to oxygen and H^- to carbon. This work has been extended to catalytic hydrosilylation, hydroboration, and ammonia borane dehydrogenation mediated by diazaphospholenes, in which the intermediacy of the corresponding free N-heterocyclic phosphenium (NHPs) demonstrates how hydridic character of P–H bonds in secondary phosphines can allow the proposed H^- shuttling in catalysis.[13a,16] The use of this "inverted" P–H bond polarization has also been demonstrated for Lewis acidic borane-mediated dehydrogenative coupling of diaryl- and arylphosphines, for which P–H hydride abstraction to give highly reactive PAr_2^+ or $P(Ar)H^+$ phosphenium is implicated.[17] However, this approach has not been explored more generally for transformations of secondary phosphines for which the corresponding phosphenium PR_2^+ fragment is less stable than the bis(amido)-substituted NHPs, or for metal-coordinated secondary phosphines.

We recently reported the synthesis of a new diarylphosphenium complex $[Mo(CO)_4(PR_2H)(PR_2)]^+$ (**1-R**, Scheme 3), which contains an ancillary secondary phosphine ligand, similar to the proposed intermediate shown prior to step A in Scheme 2.[12] We demonstrated the Lewis superacidity of the phosphenium ligand in this complex, and its ready participation in the electrophilic abstraction of F^- from $[PF_6]^-$ and H^- from Et_3SiH. Here we report the ability of **1-R** to mediate hydrophosphination of unsaturated substrates via steps A and B in the cycle shown in Scheme 2, bringing *umpolung* to this P–H addition chemistry. We also describe challenges we have identified in making these reactions chemoselective and catalytic, and preliminary attempts to address these challenges via redesign of the Mo carbonyl system.

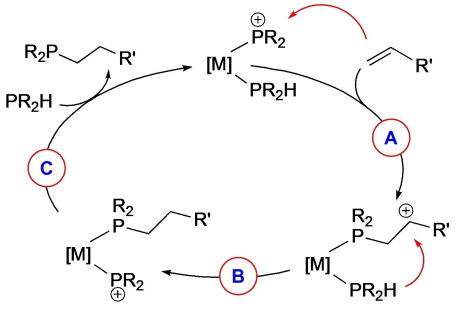

Scheme 2. Proposed outer-sphere hydrophosphination relying on electrophilic addition at a metal phosphenium intermediate and P–H hydride transfer.

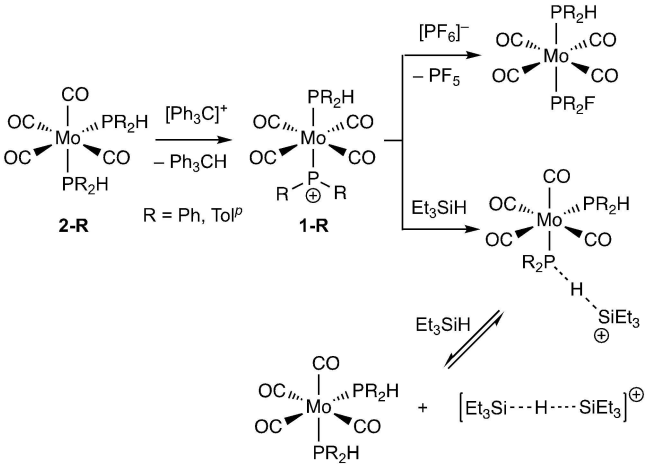

Scheme 3. Synthesis and P-electrophilic reactions of phosphenium complex **1-R**. The counteranion is $[B(m\text{-}C_6H_3Cl_2)_4]^-$, or $[BAr^{Cl}{}_4]^-$.

Results and Discussion

Addition of unsaturated substrates to $[Mo(CO)_4(PR_2H)(PR_2)]^+$ (1-R, R = Ph, Tol^p)

The addition of 1,1-diphenylethylene (**a**) or benzophenone (**b**) to a dark green solution of **1-R** in CD_2Cl_2 results in a subtle colour change to deep golden-green. NMR analysis confirms the formation of products of the general formula $[Mo(CO)_4(\mathbf{P})(PR_2)]^+$ **3-R**, where **P** is a new tertiary phosphine resulting from hydrophosphination of the C=C and C=O bonds in these substrates, respectively (Scheme 4). The new phosphenium ligands in **3-Ph-a,b** and **3-Tol^p-a,b** show diagnostic downfield $^{31}P\{^1H\}$ chemical shifts at 426.8–440.3 ppm, while peaks due to the new $PR_2(CH_2CHPh_2)$ ligands in **3-R-a** appear at 17.6–26.1 ppm and those due to $PR_2(OCHPh_2)$ in **3-R-b** appear at 132.6–134.9 ppm. $^2J_{PP}$ values of 71–89 Hz are consistent with the assignment of *trans*-**3-R** as the major product in all cases but small amounts (< 5%) of the corresponding cis isomer ($^2J_{PP}$ 31–37 Hz) are observed for **3-Ph-a,b** and **3-Tol^p-a**,b. (The preferred trans stereochemistry ensures that strongly π-acidic phosphenium ligands do not compete with CO ligands for backbonding at Mo.) The absence of P–H bonds in these new complexes is clear from their ^1H NMR spectra, which show multiplets at ~4 ppm and ~3.5 ppm due to the new P-CH_2CHPh_2 group in **3-R-a** and a doublet at ~5.7–5.8 ppm due to the P-$OCHPh_2$ group in **3-R-b**. These reactions are remarkably clean, with only minor byproducts detectable by $^{31}P\{^1H\}$ NMR (see Supporting Information). The reactions of **1-Ph** are ≥95% complete within the time taken to obtain NMR spectra (~20 min), while the reactions of **1-Tol^p** are slightly slower, ≥70% complete within this time frame.

Ethylene (**c**) also reacts with **1-R** in CD_2Cl_2 to give a hydrophosphination product, $[Mo(CO)_4(PPh_2Et)(PR_2)]^+$ (**3-R-c**), although this reaction occurs more slowly than those of the diaryl-substituted substrates **a** and **b**. Spectra recorded after 3 h show ~40% conversion of **1-Ph** to **3-Ph-c** and ~20% conversion of **1-Tol^p** to **3-Tol^p-c**. Nevertheless, given the dearth of examples of metal-catalyzed hydrophosphination of ethylene,[4h,i] this is a promising result. Again, peaks due to the new phosphenium ligands in these complexes show downfield $^{31}P\{^1H\}$ chemical shifts (433.2 ppm for **3-Ph-c**, 431.9 ppm for **3-Tol^p-c**) with large $^2J_{PP}$ of 70–71 Hz, consistent with the trans geometry shown in Scheme 4. ^1H NMR spectra show multiplets at ~1.1 ppm (CH_3) and ~2.7 ppm (CH_2) due to the new P-CH_2CH_3 groups. These reactions are very clean, with only trace byproducts observed by NMR.

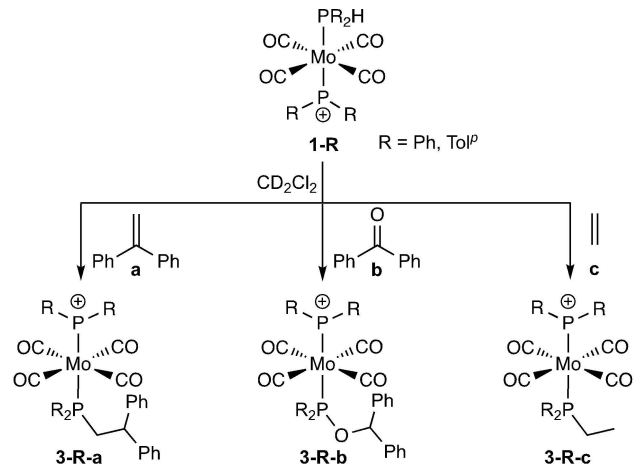

Scheme 4. Scope of stoichiometric hydrophosphination at complex **1-R**. Only the dominant trans products are shown.

We assessed the reactivity of a variety of other substrates with the strongly electrophilic complexes **1-R**, but identified no others that gave hydrophosphination products **3-R**. For example, while the aryl-substituted alkene substrates styrene and indene also react quickly with **1-R** (complete consumption of this phosphenium complex occurs within the ~20 min taken to obtain initial spectra), $^{31}P\{^1H\}$ spectra show no signals due to new phosphenium-containing complexes in the region 400–450 ppm for the reaction mixtures. Instead, signals due to multiple products appear between 50 ppm and −10 ppm (where secondary and tertiary phosphines with P–C bonds should appear), many of which correlate with signals between 125 ppm and 140 ppm (see Supporting Information). Signals in this downfield chemical shift range could correspond to bridging phosphenium ligands μ-PR_2,[18] or to new tertiary phosphines containing P–Cl bonds, although we see no evidence for such rapid reaction of the phosphenium ligand in **1-R** with solvent. For these examples hydrophosphination may be occurring (the ^1H NMR spectra show signals between 2 ppm and 4 ppm) but the phosphenium ligands in the product complexes are undergoing further reactivity, or possibly some other type of electrophilic chemistry is occurring, such as electrophilic substitution,[10] instead of the proposed hydrophosphination.

The simple alkene 1-hexene also reacts rapidly with **1-R**, with loss of $^{31}P\{^1H\}$ signals in the phosphenium region. The spectra for these reactions are less complex than those for the reactions of styrene and indene described above, being dominated by signals due to two major products. We attribute a triplet at 255 ppm and corresponding doublet at 8–9 ppm, with a cis $^2J_{PP}$ of 26–27 Hz, to a μ-PR_2-containing product with two equivalent PR_2H ligands. A $^{31}P\{^1H\}$ singlet at 8.3 ppm (reaction with **1-Ph**) or 7.6 ppm (reaction with **1-Tol^p**), which becomes a doublet with large $^1J_{PH}$~500 Hz in the ^{31}P spectrum, shows ^{31}P-^1H HMBC correlations consistent with a 2-hexenyl fragment (see Supporting Information). We have assigned this signal to the phosphonium cation $[HPR_2(2\text{-hexenyl})]^+$, which can result from intramolecular γ-deprotonation of the putative alkyl carbocation intermediate (Scheme 5). The resulting five-coordinate Mo fragment could then be trapped by complex **1-R** to generate the proposed dinuclear product.

The reaction of phenylacetylene with **1-Ph** stands out among the unsaturated substrates we investigated for giving clean conversion to a single product that does not result from hydrophosphination. Instead, a metallacyclic product, **4-Ph**, apparently results from nucleophilic attack of a Mo-bound CO ligand at the putative vinyl carbocation intermediate resulting from electrophilic addition of the phosphenium ligand in **1-Ph**

Research Article
doi.org/10.1002/chem.202302924
Chemistry Europe
European Chemical Societies Publishing

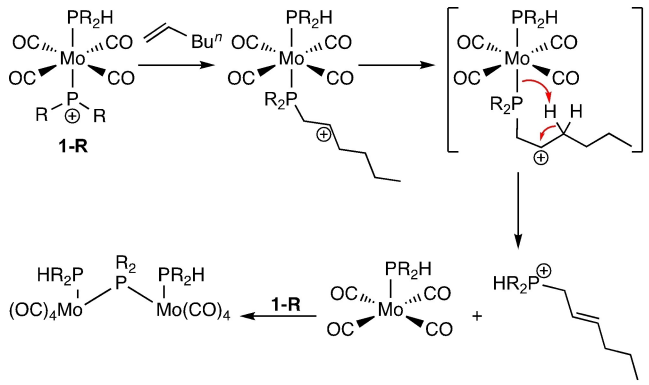

Scheme 5. Intramolecular γ-deprotonation of the carbocation resulting from reaction of 1-hexene with complex **1-R**, and subsequent trapping of the five coordinate Mo byproduct by **1-R**.

at the alkyne (Scheme 6). Complex **4-Ph** is red, instead of the deep golden-green colour observed for the hydrophosphination products **3-R-a**–**c** described above, consistent with an oxidation state change (Mo^0 to Mo^{II}) that accompanies this transformation. Multinuclear 2D NMR characterization supports the unusual structure shown in Scheme 6 (see Supporting Information for full details). $^{13}C\{^1H\}$ NMR is particularly diagnostic, including three peaks due to Mo-bound carbonyl groups at 266.4 ppm, 218.8 ppm and 202.8 ppm. Each of these appears as a doublet of doublets due to coupling to two inequivalent P, with $^2J_{PC}$ consistent with the expected cis and trans relationships shown for **4-R** in Scheme 6. The downfield carbonyl signal at 266.4 ppm is within the normal ^{13}C range for Mo-bound acyl ligands,[19] and shows a three-bond correlation with a unique alkene ^1H signal at 9.24 ppm – strong evidence for the new C–C bond that has formed in **4-Ph**. Complex **1-Tol^p** reacts with phenylacetylene to give the same colour change to red and comparable NMR spectra. Rapid trapping of these vinyl carbocation intermediates by the nearest nucleophile is consistent with their much lower stability, relative to the secondary or tertiary alkyl carbocations resulting from phosphenium addition to alkenes. Comparable intramolecular reactivity was reported, and studied computationally, for the addition of alkynes to W-bound phosphenium ligands; in that case the vinyl carbocation intermediates were trapped by electron-rich P-substituents.[10c] Here, formation of **4-R** highlights the possible timescale of rearrangement at Mo required to access the hydridic P–H bond in this system, subsequent to electrophilic addition to the alkyne (vide infra).

Finally, the addition of methyl acrylate, an electron-deficient alkene that readily undergoes metal-catalyzed hydrophosphination involving nucleophilic metal phosphido intermediates,[4i,20] gives no reaction with **1-R** on the timescale of the other reactions described above.[21] This provides indirect support for the electrophilic addition mechanism for hydrophosphination that we have proposed for this system.

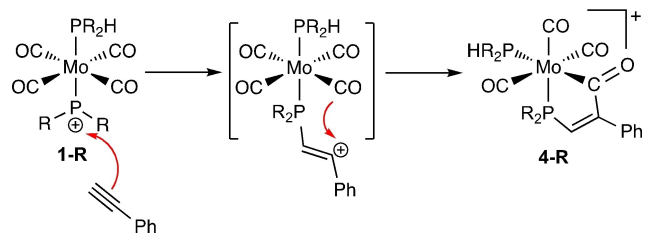

Scheme 6. Reaction of phenylacetylene with complex **1-R**, including proposed fundamental steps leading to metallacyclic product **4-R** (R = Ph, Tol^p).

Mechanistic aspects of the reactions of unsaturated substrates with $[Mo(CO)_4(PR_2H)(PR_2)]^+$ (1-R)

We have proposed that the stoichiometric hydrophosphination reactions shown in Scheme 4 proceed via electrophilic addition of the phosphenium ligand in **1-R** to alkene and ketone functionalities to give P-bound carbocationic intermediates, followed by intramolecular hydride transfer from a coordinated secondary phosphine ligand, which regenerates a reactive phosphenium ligand in the products (Scheme 7). Certainly the products observed for the reactions of **1-R** with benzophenone (**3-R-b**, P–O bond formation), 1-hexene, and phenylacetylene (**4-R**) are consistent with a mechanism relying on electrophilic addition, as is the absence of reaction with methyl acrylate. For the subsequent intramolecular hydride "quenching" to take place, isomerization of the two P-ligands from trans (in **1-R**) to cis must occur. (Further isomerization is then required to give the observed *trans*-**3-R** products.) This is certainly plausible – although we have shown **1-R** here as its trans isomer, it exists in solution as a 95 : 5 mixture of trans and cis isomers, and in other reactivity studies we often observe dominant cis stereochemistry in Lewis adducts of **1-R** or products of electrophilic abstraction by the phosphenium ligand.[12,22] This may be driven by a decrease in the π-acidity of the PR_2 fragment, relative to the ancillary CO ligands, during this P-element bond formation. The rate at which isomerization occurs may be relevant to the

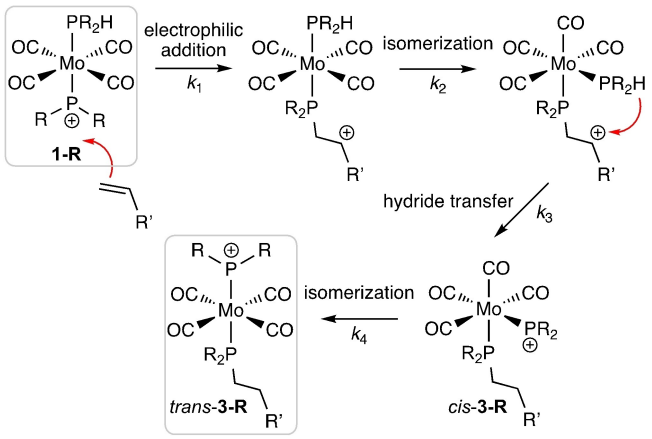

Scheme 7. Proposed stepwise mechanism for stoichiometric hydrophosphination of unsaturated substrates at complex **1-R**, shown for a generic terminal alkene.

chemoselectivity (or lack thereof) that we observe in these reactions of unsaturated substrates.[23]

Alternate reactivity to the desired hydrophosphination could occur at several points in the mechanism shown in Scheme 7. For example, it is possible that allylic hydride abstraction from indene or 1-hexene could compete with the initial electrophilic addition step (k_1),[24] although the simple product mixtures observed for the reactions of 1-hexene with **1-R** suggest this is not happening, at least for that substrate. A larger issue in the selective formation of hydrophosphination product **3-R** is the possibility of reactions that compete with intramolecular hydride transfer at the carbocation intermediates if the trans to cis isomerization is slow (k_2), or if the rate of hydride transfer itself is slow relative to these alternative processes (k_3). The reaction of **1-R** with phenylacetylene is an example of the outcome when isomerization/hydride transfer is slow relative to competing nucleophilic addition of CO at the trans carbocation intermediate. The two gem-diaryl substrates, 1,1-diphenylethylene and benzophenone, probably react cleanly to give hydrophosphination products **3-R** because each will react with the phosphenium ligand to give tertiary carbocations stabilized by two adjacent phenyl groups. These evidently have sufficient lifetimes to allow both isomerization and P–H hydride transfer. The analogous electrophilic addition of ethylene will give a far more reactive carbocation, but its simplicity limits alternative chemistry to the hydride transfer reaction leading to hydrophosphination, whereas the presence of the alkyl sidechain at the putative carbocation resulting from electrophilic addition at 1-hexene allows γ-deprotonation to occur.[25] Finally, the phosphenium ligand in **3-R** is still a highly electrophilic species that may participate in further reactivity precluding the clean formation of **3-R**. Our previous experimental and computational studies have shown that the phosphenium ligand in *cis*-**1-R** is more Lewis acidic than that in *trans*-**1-R**, presumably because it is trans to a CO ligand in the cis isomer, and competing for π-backbonding at Mo.[12] If the final cis/trans isomerization step in Scheme 7 is slow (k_4), this may be responsible for some of the reaction mixtures for which we no longer see signals in the terminal phosphenium region.

DFT analysis provides evidence for the proposed intramolecular hydride transfer from coordinated secondary phosphine to an intermediate carbocation, and suggests that its rate is indeed limited by structural rearrangement such as the isomerization from trans to cis geometry at Mo (e.g. k_2 in Scheme 7). Trajectories for the addition of two representative alkenes, styrene and ethylene, to the cis isomer of **1-Ph** were assessed. For styrene, the intermediate carbocation adduct was located, as well as the transition state between this intermediate and the final hydrophosphination product (Figure 2a), which corresponds to a low barrier of 7 kcal/mol for hydride transfer from the cis secondary phosphine ligand. If we assume initial adduct formation occurs at the dominant trans isomer of **1-Ph** as shown in Scheme 7, these results suggest the timescale for trans/cis isomerization of the intermediate carbocation adduct is long relative to the hydride transfer, which allows the intermediate to participate in other reactions, as observed experimentally. Indeed, several other conformers of the coordinated phosphacarbocation intermediate were also located, all within 1 kcal/mol of the energy of the "productive" conformer, a factor that would allow this alternate reactivity. In contrast to the results for styrene, no intermediate carbocation adduct could be located for the reaction of ethylene with **1-Ph**, which is consistent with the anticipated instability of this primary carbocation. Instead, the calculations show that hydrophosphination of ethylene at *cis*-**1-Ph** occurs in a concerted fashion from an encounter complex of appropriate conformation, via a single transition state (Figure 2b). The calculated $\Delta G^{\ddagger}$ of ~16 kcal/mol is considerably higher than the electronic energy barrier of ~4 kcal/mol, which likely reflects a high entropic component imposed by the very specific conformational requirements of this transformation.

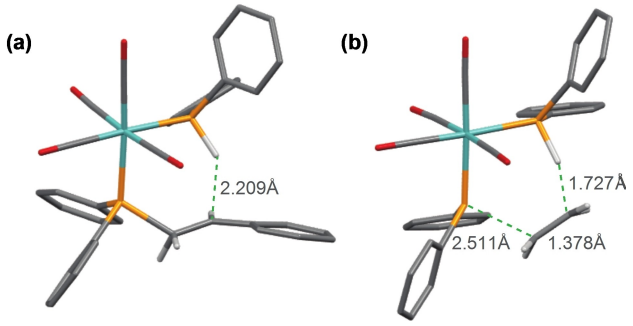

Figure 2. (a) Calculated transition state for intramolecular hydride transfer from Mo-PPh_2H to the intermediate phosphacarbocation resulting from addition of styrene to *cis*-**1-Ph** (k_3 in Scheme 7). (b) Calculated transition state for hydrophosphination of ethylene at *cis*-**1-Ph** via concerted electrophilic attack of Mo-PPh_2^+ and intramolecular hydride transfer from Mo-PPh_2H. Aromatic C–H groups have been omitted for clarity.

These DFT results show that the proposed intramolecular hydride transfer step is reasonable if geometric isomerism can occur. However, it is possible to envisage alternative, intermolecular pathways. For example, transfer might occur from a second molecule of the trans carbocation intermediate (Scheme 8a). To probe this possibility, we carried out a 1 : 1 reaction of **1-Ph** with 1,1-diphenylethylene in the presence of the bis(phosphine) precursor *cis*-$Mo(CO)_4(PPh_2H)_2$ (**2-Ph**), a potential external hydride donor (Scheme 8b). If an intramolecular mechanism is responsible for the hydride transfer step during hydrophosphination of 1,1-diphenylethylene at **1-Ph**, we would expect the products to include exclusively **3-Ph-a**, along with unreacted **2-Ph**. If intermolecular hydride transfer is occurring, we should see a new, neutral complex **5-Ph-a**, containing both PPh_2H and the hydrophosphination product as ligands, along with **1-Ph** (newly formed by loss of H^- from **2-Ph**). Ultimately, the reaction mixture contained products resulting from both these pathways: we see an approximately equimolar mixture of **3-Ph-a** and a new complex we have assigned as the cis isomer of **5-Ph-a**. Complex **5-Ph-a** shows $^{31}P\{^1H\}$ signals at 31.5 ppm and 18.7 ppm with $^2J_{PP}$ 27 Hz, and ^{31}P NMR confirms the signal at 18.7 ppm is due to a ligand containing a P–H bond. The ^1H NMR spectrum shows new methine and methylene signals at ~4.5 and ~3.3 ppm, respectively, due to the coordinated hydrophosphination product in **5-Ph-a**, distinct from the correspond-

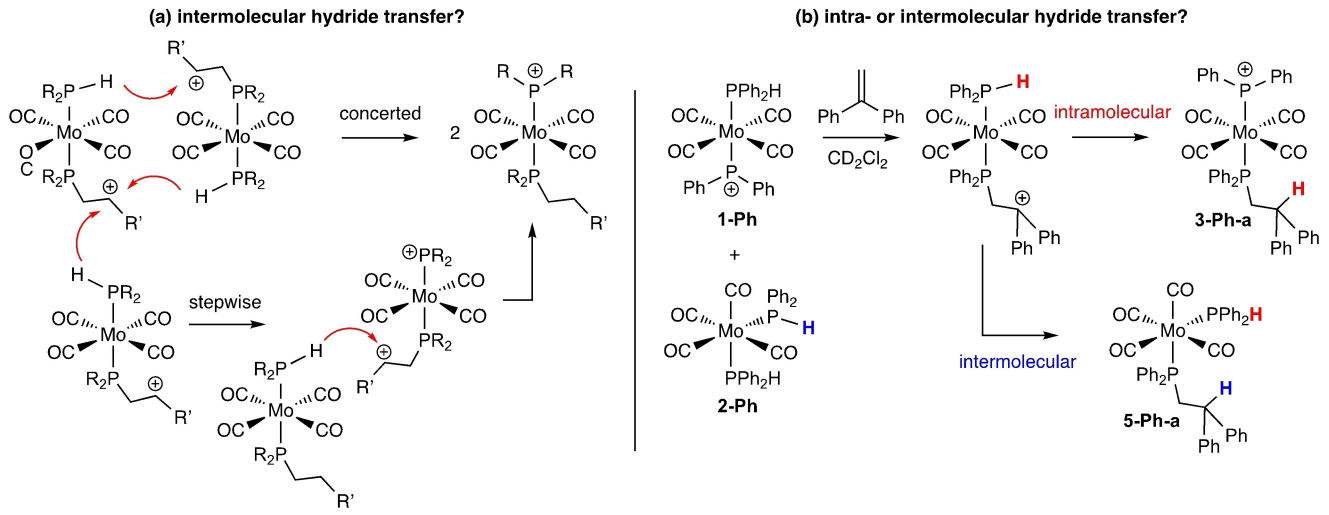

Scheme 8. (a) Possible intermolecular hydride transfer mechanisms for the stoichiometric hydrophosphination of unsaturated substrates at complex **1-R**, and (b) an experiment probing whether intra- or intermolecular hydride transfer is occurring.

ing signals at ~4.2 ppm and 3.6 ppm, respectively, for **3-Ph-a**. Thus, this experiment suggests that both intra- and intermolecular hydride transfer are possible. However, we note that the neutral bis(phosphine) complex **2-Ph** is a good hydride donor that could bias the reaction toward intermolecular hydride transfer.[12] In the absence of **2-Ph**, only the cationic species shown in Scheme 8a, or the phosphenium complex **1-Ph**, would have P–H bonds available, and these would be less effective hydride donors (e.g. δ^1H_{PH} for **1-Ph** is 7.13 ppm, while for **2-Ph** it is 5.96 ppm). For example, we established that complex **1-Ph** does not react with trityl cation to give the dicationic bis(phosphenium) complex $[Mo(CO)_4(PPh_2)_2]^{2+}$ on the timescale of the observed hydrophosphination reactions, so it seems unlikely that this complex will transfer a hydride to a reactive carbocation.[26] Further mechanistic analysis relevant to the nature of the proposed hydride transfer step is described in a subsequent section.

Synthesis of more electron-rich phosphenium complexes $[Mo(CO)_3(PR_2H)_2(PR_2)]^+$ (7-R)

As noted above, the complex reaction mixtures or selectivity for non-hydrophosphination products that we observe for the addition of a number of unsaturated substrates to complex **1-R** could derive from the very strong Lewis acidity and corresponding electrophilicity exhibited by the phosphenium ligand in this complex, or from slow hydride transfer to the proposed reactive carbocation intermediates. One way to adjust both the reactivity at the phosphenium and the hydricity of the remaining P–H bond in a coordinated secondary phosphine ligand is to tune the "ancillary" Mo fragment, to make it more electron-rich. To investigate the impact of such electronic tuning, we prepared new phosphenium complexes in which one CO ligand has been replaced with a second secondary phosphine ligand, $[Mo(CO)_3(PR_2H)_2(PR_2)]^+$ ([**7-R**][B(*m*-$C_6H_3Cl_2)_4$]), by hydride abstraction from the *fac*-tris(phosphine) precursors **6-R** (Scheme 9).

The new phosphenium complexes **7-Ph** and **7-Tol^p** are isolated as green powders. $^{31}P\{^1H\}$ NMR of **7-R** show diagnostic downfield signals corresponding to a phosphenium ligand (396 ppm (**7-Ph**), 392 ppm (**7-Tol^p**)) and signals due to two inequivalent secondary phosphine ligands (from 2.8 ppm to 7.1 ppm), consistent with the mer configuration shown in Scheme 9. These phosphenium $^{31}P\{^1H\}$ chemical shifts are significantly upfield relative to those for **1-Ph** and **1-Tol^p**, which appear at 441 ppm and 439 ppm, respectively. This is consistent with a more electron-rich coordination environment in **7-R**. Likewise, in the ^1H NMR the secondary phosphine P–H signals for **7-R** appear between 6.35 ppm and 6.59 ppm, upfield from (and more hydridic than) those for **1-Ph** and **1-Tol^p** (7.13 ppm and 7.06 ppm, respectively). Accordingly, the effective Lewis acidities of the new phosphenium complexes **7-R**, as determined by Gutmann-Beckett experiments,[27] are significantly lower than those for the Lewis superacidic complexes **1-Ph** and **1-Tol^p**, for which the observed shift in $\delta^{31}P$ values for triethylphosphine oxide on binding to the phosphenium ligand are 45.4 ppm and 44.4 ppm, respectively. The $\Delta\delta^{31}P$ values of 23.3 ppm (**7-Ph**) and 23.0 ppm (**7-Tol^p**) are much closer to that for the Lewis acid catalyst $B(C_6F_5)_3$ ($\Delta\delta^{31}P$ 27.0 ppm).[28] Thus, the new phosphenium complexes are still reasonably strong Lewis acids, so we would expect them to exhibit electrophilic reactivity, but it should be tempered relative to the reactivities

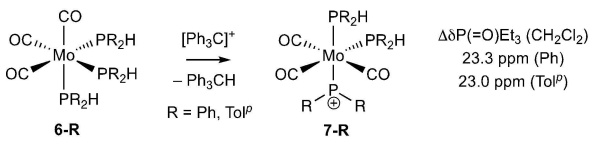

Scheme 9. Synthesis of $[Mo(CO)_3(PR_2H)_2(PR_2)]^+$ (**7-R**) and its effective Lewis acidity as determined from Gutmann-Beckett experiments. The counteranion is [B(*m*-$C_6H_3Cl_2)_4]^-$.

observed for **1**-**R**. Notably, the geometry of **7**-**R** ensures the presence of a secondary phosphine ligand cis to the reactive phosphenium ligand, removing the requirement for isomerization at Mo prior to P–H hydride transfer to the carbocation adducts formed during hydrophosphination.

Addition of unsaturated substrates to $[Mo(CO)_3(PR_2H)_2(PR_2)]^+$ (7-R)

1,1-diphenylethylene (**a**), benzophenone (**b**), and ethylene (**c**) all react with **7**-**R** to give hydrophosphination products as they did with **1**-**R** (Scheme 10). Stepwise hydrophosphination of two equivalents of each substrate is observed because **7**-**R** contains two secondary phosphine ligands, both with P–H bonds available as sources of hydride. The first hydrophosphination results in a pair of mer isomers of $[Mo(CO)_3(\mathbf{P})(PR_2H)(PR_2)]^+$, **8**-**R**, (in an approximate 1 : 1 ratio) in which the hydrophosphination product ligand (**P**) is either cis or trans to the new phosphenium ligand, as determined by $^{31}P\{^1H\}$ NMR. These generally react with a second equivalent of substrate to generate two mer isomers of the bis(hydrophosphination) product complex $[Mo(CO)_3(\mathbf{P})_2(PR_2)]^+$, **9**-**R**. The dominant isomer of **9**-**R** contains the two **P** ligands trans to each other and cis to the new phosphenium ligand.[29] This contrasts with the usual preference of π-acidic PR_2^+ to be trans to a phosphine ligand instead of a CO ligand (for example as we see for the hydrophosphination reactions at **1**-**R**, vide supra). Steric congestion in **9**-**R** probably disfavours the structure of the minor isomer (as well as a fac isomer), which places the two bulky hydrophosphination product ligands cis to one another (one trans and one cis to the phosphenium ligand). However, kinetic selectivity for the formation of *trans*-**9R** could also influence this distribution: the adjacent phosphenium and secondary phosphine ligands in *trans*-**8**-**R** allow electrophilic addition and subsequent P–H hydride transfer to access *trans*-**9**-**R** directly, without any rearrangement, while *cis*-**8**-**R** must isomerize to allow hydride transfer to a putative carbocation. $^{31}P\{^1H\}$ NMR signals for the phosphenium ligands in complexes **8**-**R** and **9**-**R** appear at 380–396 ppm, while those due to coordinated hydrophosphination products appear at 20–44 ppm (new P–C bonds) or 136–144 ppm (new P–O bonds) and coordinated PR_2H in **8**-**R** appear at 4–10 ppm.

The reaction of 1,1-diphenylethylene with **7**-**Ph** is much slower than the analogous reaction with **1**-**Ph**, giving almost complete conversion to **9**-**Ph**-**a** after 2 d, with some residual **8**-**Ph**-**a**. The reaction with **7**-**Tol**^{p} is even slower – after 10 d there is still a mixture of **8**-**Tol**^{p}-**a** and **9**-**Tol**^{p}-**a**. Benzophenone reacts more quickly, although still more slowly than with **1**-**R**: conversion to the double hydrophosphination product **9**-**Ph**-**b** is complete within ~2 h, while the reaction with **7**-**Tol**^{p} is complete within 24 h. We would expect the C=O moiety in benzophenone to be a better nucleophile for the phosphenium ligands in **7**-**Ph** and **8**-**Ph**-**b** than the C=C bond in 1,1-diphenylethylene, so these results may indicate that electrophilic addition is rate-limiting in this reaction, at least for 1,1-diphenylethylene (vide infra). This would certainly be consistent with reduced Lewis acidity of the phosphenium ligand in **7**-**R**. Although the challenges of adding stoichiometric amounts of ethylene make it difficult to compare its rates of reaction across samples, this hydrophosphination chemistry does not appear to be significantly slower at **7**-**R** than at **1**-**R**.

As shown in Scheme 10, a much wider range of unsaturated substrates participate in the desired P–H addition chemistry at **7**-**R** than those that underwent hydrophosphination at **1**-**R**. Styrene (**d**), indene (**e**), and 1-hexene (**f**) now also undergo relatively clean stoichiometric hydrophosphination to give one or both of **8**-**R** and **9**-**R**, as determined by $^{31}P\{^1H\}$ and ^1H NMR. As for 1,1-diphenylethylene, these substrates react much more slowly with **7**-**R** than they do with **1**-**R**, and the reactions of **7**-**Tol**^{p} are slower than those of **7**-**Ph**. The reactions of 1-hexene are especially slow: for **7**-**Ph** approximate 1 : 1 mixtures of **8**-**Ph**-**f** and **9**-**Ph**-**f** persist after 7 d, and **7**-**Tol**^{p} does not react completely even after 14 d, with only **8**-**Tol**^{p}-**f** and no **9**-**Tol**^{p}-**f** being formed. On the other hand, the nucleophilic dialkylketone cyclohexanone reacts exceptionally quickly with **7**-**Ph**, giving complete conversion to **9**-**Ph**-**g** within 20 min, and within hours with **7**-**Tol**^{p} to give **9**-**Tol**^{p}-**g**.

Not all the unsaturated substrates we added to **7**-**R** gave hydrophosphination products **8**-**R** and **9**-**R**. As for **1**-**R**, we see no reaction of **7**-**R** with the electron-deficient alkene methyl acrylate. No reaction was observed for *trans*-stilbene, cyclohexene, or *cis*-butene, which points to likely steric constraints

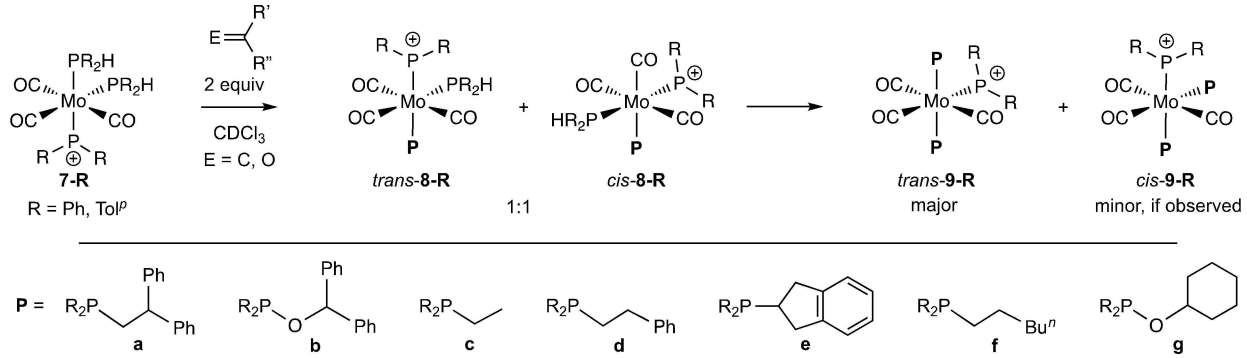

Scheme 10. Scope of hydrophosphination reactivity at **7**-**R**. The cis/trans labels for intermediate **8**-**R** refer to the relative positions of the hydrophosphination product (**P**) and phosphenium ligands. The cis/trans labels for **9**-**R** refer to the relative positions of the two hydrophosphination product (**P**) ligands.

for the addition of internal alkenes to the phosphenium ligand in **7-R**. Addition of the electron-rich alkene vinyl ether caused the NMR sample to become viscous within 5 min, which suggests the alkene was polymerized – a clear limitation of the involvement of a cationic complex in the desired hydrophosphination reaction.[30] Finally, the reaction of phenylacetylene with **7-Ph** gives $^{31}P\{^1H\}$ signals consistent with formation of a metallacyclic complex analogous to **4-R** (Scheme 6), containing a metal acyl functionality: $[Mo(CO)_2(PPh_2H)_2\{\kappa^2\text{-}\underline{P}Ph_2CHCPh\underline{C}(O)\}]^+$ (**10-Ph**). For this alkyne substrate it seems the highly unstable sp^2-carbocation is inevitably intercepted through nucleophilic attack by a Mo-bound carbonyl group.

Mechanistic aspects of the reactions of unsaturated substrates with $[Mo(CO)_3(PR_2H)_2(PR_2)]^+$ (7-R)

Although lower P-electrophilicity in **7-R** (and **8-R** and **9-R**) should limit undesired additional reactivity of the phosphenium ligands in this system, the high selectivity we see for hydrophosphination products in the reactions of **7-R**, relative to the reactions of **1-R**, probably results primarily from faster "quenching" of the highly reactive carbocation intermediates by hydride transfer from the available P–H groups, preventing their participation in undesired side reactions. As noted above, these are more hydridic in **7-R** than in **1-R**, and, because one of the two PR_2H ligands is cis to the reactive phosphenium ligand in **7-R**, no ligand rearrangement is needed prior to quenching.

The first step of the proposed hydrophosphination mechanism for **7-R** (conversion to **8-R**) is shown in Scheme 11. The lower electrophilicity of the phosphenium ligand is likely responsible for the generally slower rates of reaction of **7-R** relative to **1-R**, and for the fact that **7-Tol**^{p} reacts more slowly than **7-Ph**.[31] This initial, electrophilic addition step (k_1) could be rate-limiting for all substrates, if hydride transfer step (k_2) is very fast. The very low calculated barrier for this transfer in the carbocationic styrene adduct of *cis*-**1-Ph**, suggests that this may indeed be the case for the reactions of **7-R**. However, the hydrophosphination reactions occur very quickly for the alkyl

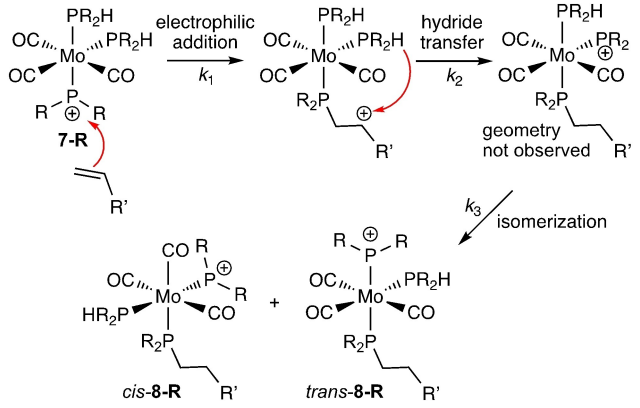

Scheme 11. Proposed mechanism for hydrophosphination of unsaturated substrates by bis(phosphine) phosphenium complex **7-R**. The first of the two possible hydrophosphinations is shown, for a generic alkene substrate.

ketone substrate cyclohexanone, which is an excellent nucleophile for the phosphenium ligands. In this case, the rate-limiting step could be hydride transfer, even though it is likely to be occurring faster for this system than for **1-R**.

The cleaner, slower reactions of unsaturated substrates at **7-R** provided an opportunity to obtain rate data by NMR monitoring. For example, we used ^1H NMR to obtain a room temperature rate constant for the disappearance of **7-Ph** in the hydrophosphination of styrene ($k = 0.079\ M^{-1}\,s^{-1}$). This allowed us to calculate an approximate Mayr electrophilicity parameter for **7-Ph** of $E = -1.94$ (see Supporting Information).[32] This value places the cationic, Mo-bound diphenylphosphenium ligand in **7-Ph** among the more electron-rich benzhydrylium reference electrophiles in the Mayr scale: it is a weaker electrophile than $[(p\text{-}C_6H_4OMe)_2CH]^+$ ($E = 0$) but stronger than $[(p\text{-}C_6H_4NPh_2)CH]^+$ ($E = -4.72$). In this context, the very slow reaction of **7-Ph** with 1-hexene is consistent with its nucleophilicity parameter of $N = -2.25$, which is approximately four units higher on the Mayr scales than **7-Ph**,[32c] while faster reactions are seen for the better-matched nucleophiles styrene ($N = 0.78$) and phenylacetylene ($N = 0.34$).

We carried out Variable Time Normalization Analysis (VTNA) to obtain an experimental rate law for the hydrophosphination of styrene by complex **7-Ph**. We hoped that this experiment would tell us about the hydride transfer step in these reactions, because a second order rate dependence on [**7-Ph**] would provide evidence for *inter*molecular quenching of the carbocation intermediate (vide supra). However, the VTNA analyses showed that the reaction rate has first order dependence on both [**7-Ph**] and [alkene]. This result is consistent either with a mechanism involving intermolecular hydride transfer in which electrophilic addition is rate-limiting, or with a mechanism involving intramolecular hydride transfer in which either electrophilic addition or hydride transfer is rate-limiting.

We also used ^1H NMR monitoring to carry out a Hammett analysis, measuring the rates of hydrophosphination for a series of *para*-substituted styrene derivatives (Figure 3). This experiment was intended to confirm that the observed hydrophosphination chemistry results from the proposed electrophilic addition chemistry, in which case we would expect a linear Hammett plot consistent with the impact of the alkene *para*-substituents on the rate of the reaction.

Figure 3a shows the resulting Hammett plot, which is not linear. However, it does show correlations, with a "concave upward" deviation from linear. The slopes on both sides of the inflection are negative, which is consistent with a buildup of positive charge at the benzylic carbon of the styrene derivatives in the transition state for the relevant rate-determining step(s). Such a change in slope could be due to a change in the hydrophosphination mechanism along the series of substrates, or to a change in rate-determining step within a common, multistep mechanism such as the proposed mechanism shown in Scheme 11. Addition to an electropositive phosphenium ligand (k_1) will certainly involve an increase in positive charge at the benzylic carbon on the styrene (Figure 3b, top). On the other hand, hydride transfer to the carbocation in this reaction (k_2) requires hydridic P–H bond polarization, which is also

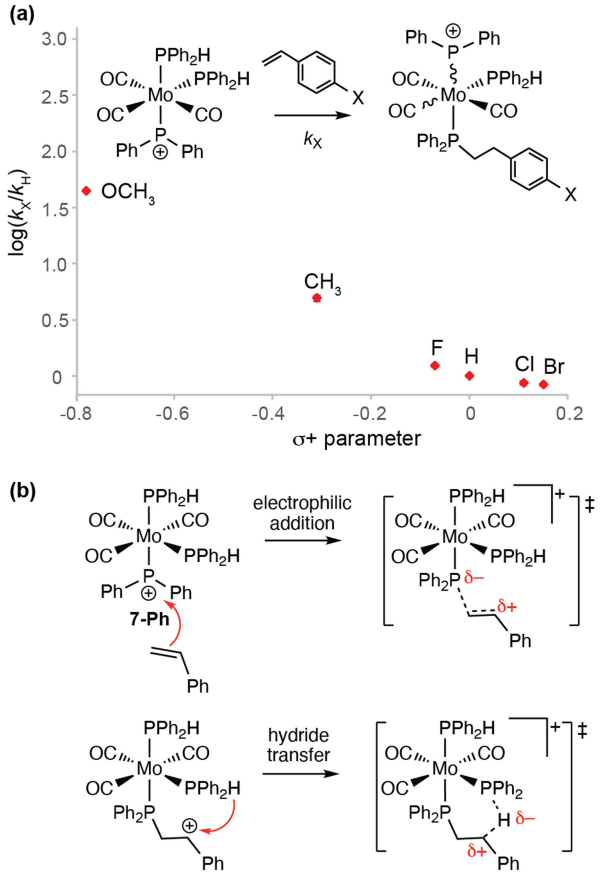

Figure 3. a) Hammett plot for the reaction of *para*-substituted styrenes with **7-Ph**. Rates were measured for the disappearance of **7-Ph**. Error bars for triplicate runs are included except for X = OCH_3 and are on the order of the size of the data points. The reaction of *p*-methoxy styrene is complete before we can record the first NMR spectrum, so the value of k_{OMe} is an estimated lower limit. b) Steps in the proposed mechanism for hydrophosphination of styrenes by complex **7-R** for which a build-up of positive charge occurs at the benzylic carbon in the transition state.

arguably impacted by the degree of positive charge localized at the benzylic carbon (Figure 3b, bottom). As discussed above, we expect that electrophilic addition is slower and rate-determining for the reaction of most substrates with **7-Ph**, although we cannot rule out the possibility that hydride transfer is rate-limiting for the most electron-rich, nucleophilic styrenes in this study. Alternatively, a second, concerted hydrophosphination mechanism, comparable to the trajectory we observe computationally for the addition of ethylene to complex **1-Ph** (vide supra), could be in effect for the less electron-rich styrene substrates.

Preliminary reactivity studies relevant to catalysis

The addition of excess PPh_2H and unsaturated substrates (as 1:1 mixtures) to these phosphenium complexes does not result in the release of free hydrophosphination product **P** and regeneration of **1-Ph** or **7-Ph**, as would be expected if the simple catalytic cycle shown in Scheme 2 is in operation. Instead, more complex reaction mixtures result, which involve one or more exchange processes, as determined by $^{31}P\{^1H\}$ NMR. Preliminary control reactions have allowed the identification of some of these species.

The addition of a 1:1 mixture of PPh_2H and 1,1-diphenylethylene to **1-Ph** gives a colour change to yellow. The hydrophosphination product $PPh_2CH_2CHPh_2$ (**P**) is not observed in the reaction mixture, either as the free phosphine (as we had expected) or coordinated to Mo in $[Mo(CO)_4(\mathbf{P})PR_2]^+$ (**3-R-b**).[33] Instead we observe signals due to a new complex, **11-Ph**, in which the secondary phosphine substrate has formed an adduct with the phosphenium ligand in **1-Ph** (Scheme 12), along with small amounts of $Mo(CO)_4(PPh_2H)_2$ (**2-Ph**) and $Mo(CO)_3(PPh_2H)_3$ (**6-Ph**). Complex **11-Ph** can also be generated cleanly by the addition of an equivalent of PPh_2H to **1-Ph** in the absence of alkene. In both samples, the P-bound PPh_2H appears in the $^{31}P\{^1H\}$ NMR as a sharp doublet at −3.4 ppm with $^1J_{PP}$ 243 Hz, while the former phosphenium ligand gives a corresponding, broad doublet at 82.2 ppm.[34] The signal due to the Mo-bound PPh_2H ligand at 15.4 ppm is also broadened, but trans $^2J_{PP}$ coupling of 65 Hz is discernible. These $^{31}P\{^1H\}$ spectra also show a broadened signal at about −37.7 ppm that is apparently due to free PPh_2H undergoing exchange with the Mo-bound PPh_2H trans to the new adduct ligand. Thus, 1,1-diphenylethylene does not compete with secondary phosphine for binding at the strongly Lewis acidic PPh_2^+ ligand in **1-Ph** under these "pseudo-catalytic" conditions.

We repeated the above reactions in a stepwise fashion, generating the hydrophosphination product **3-Ph-a** in situ from the addition of alkene to **1-Ph**, then adding an equivalent of PPh_2H to see if the product phosphine **P** could be substituted. This resulted in formation of another adduct complex, **12-Ph**, with PPh_2H bound to the phosphenium ligand in **3-Ph-a** (again along with small amounts of the phosphine complexes **2-Ph** and **6-Ph**). $^{31}P\{^1H\}$ signals for complex **12-Ph** are almost identical to those for **11-Ph**, except that the broad doublet due to the trans $PPh_2CH_2CHPh_2$ ligand appears at 34.1 ppm, much further downfield than the signal due to the trans PPh_2H ligand in **11-Ph**. This spectrum again includes a broad signal at −37.0 ppm,

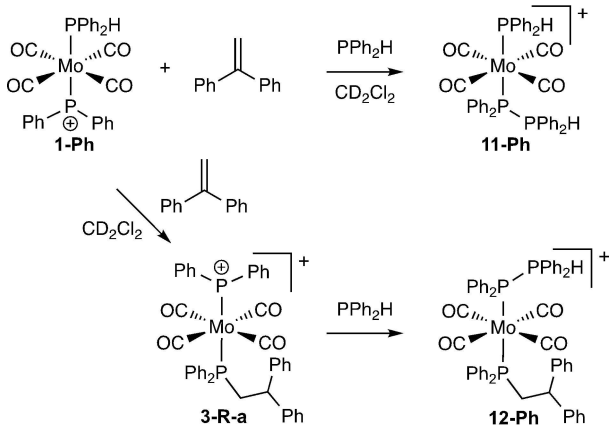

Scheme 12. Reactions of **1-Ph** with 1,1-diphenylethylene and PPh_2H.

which suggests that free PPh_2H is undergoing exchange with the Mo-bound **P**.

The analogous series of experiments for the less electrophilic **7-Ph** (using styrene instead of 1,1-diphenylethylene because it reacts more quickly) gives more complex reaction mixtures (see Supporting Information). We have tentatively assigned $^{31}P\{^1H\}$ NMR signals observed for a mixture of two equivalents of PPh_2H with **7-Ph** to two isomers of the complex **13-Ph**, which again contain PPh_2H bound to the phosphenium ligand (Scheme 13). However, there is clearly significant exchange occurring in this sample: peaks due to the former PPh_2 ligand are barely discernible as a broad lump in the baseline at 133.0 ppm, and among the several multiplets due to PPh_2H appearing at 10–26 ppm, none exhibit $^1J_{PP}$ coupling. Like the spectra for the simpler adduct complexes **11-Ph** and **12-Ph**, a broad peak apparently due to free PPh_2H participating in exchange at **13-Ph** appears at −29.7 ppm. The breadth and downfield shift of the (former) phosphenium PPh_2 peak suggest that adduct formation is reversible on the NMR timescale.

An almost identical $^{31}P\{^1H\}$ spectrum is obtained for the addition of two equivalents of a 1:1 mixture of styrene and PPh_2H to **7-Ph** (just one dd shifts from 24 ppm to 21 ppm); it is unclear whether the apparently reversible PPh_2H adduct formation has allowed any hydrophosphination of styrene to occur (we see no signals due to free $PPh_2CH_2CH_2Ph$).[33] An even more complex product mixture results from the addition of two equivalents of PPh_2H to a mixture of the hydrophosphination products **8-Ph-d** and **9-Ph-d** generated in situ, of which the most notable feature is the persistence of $^{31}P\{^1H\}$ signals due to **9-Ph-d**. Overall these reactions of **7-Ph** suggest that phosphine adduct formation at the reactive phosphenium ligands in this system is not inevitable and may be reversible, which is encouraging in the context of allowing possible alkene reactivity with **7-R** in the presence of substrate phosphine. Indeed, there is precedent for the reversible coordination of phosphines to metal-coordinated phosphenium ions,[10e] and the lability of the P–P bond in free "phosphinophosphonium" cations $[R_3P\text{-}PR'_2]^+$ is well established.[35] Further studies of these Mo-bound adducts and their reactivity are currently in progress. These should inform as to the reaction conditions and complex (re)design needed to effect catalysis.

Conclusions

We have shown that the electrophilicity of metal-coordinated phosphenium ligands can be harnessed in concert with the hydride donor ability of metal-coordinated diarylphosphine ligands to allow a novel, outer-sphere, hydrophosphination reaction for a range of unsaturated substrates, including the simple alkenes ethylene and 1-hexene. These results provide proof of concept for potential P ligand-centered, electrophilic hydrophosphination catalysis. This is a new paradigm within the field of metal-catalyzed hydrophosphination, reminiscent of the Tilley-Glaser hydrosilylation mechanism, which relies on the addition of unsaturated substrate at an electrophilic Ru silylene ligand.[36] It brings the promise of substrate complementarity to established nucleophilic catalysis, which generally operates only for activated, electron-deficient unsaturated substrates.

Similarly, the challenges presented by the design of electrophilic hydrophosphination catalysts are complementary to those presented by nucleophilic catalysts. For example, reactive phosphacarbanion intermediates in outer-sphere, nucleophilic hydrophosphination catalysis can initiate competing polymerization of activated alkene substrates (analogous to the cation-initiated polymerization of electron-rich vinyl ether we observe in the chemistry of **7-R**) or participate in nucleophilic addition at ancillary ligands (like the electrophilic addition of vinyl carbocations we observe at Mo-CO ligands), leading to catalyst deactivation or poisoning. However, the widespread use of nucleophilic hydrophosphination catalysis shows that such competing reactivity can be reduced, or removed entirely, with appropriate catalyst design and optimization of reaction conditions.[7a] This should be possible also for the proposed electrophilic catalysis.

Our exploration of the reactivity of the two simple Mo(0) complexes **1-R** and **7-R** demonstrates that the electrophilic reactivity of phosphenium ligands can be manipulated through variation of the ancillary metal complex. It is quite remarkable that such a small change in complex structure can lead to increased selectivity for straightforward P–H addition, among the variety of electrophilic processes unleashed by the addition of unsaturated substrates to these cationic complexes. The ability to tune the electronic and steric environment at these metal fragments is likely to be critical to extension of the observed stoichiometric hydrophosphination to systems exhibiting catalytic turnover, especially since our investigations suggest that phosphine adducts of the active phosphenium ligands dominate under catalytic conditions. The balance of phosphenium electrophilicity and steric access required to encourage reversibility of phosphine-phosphenium adduct formation, while still allowing nucleophilic attack by the alkene substrate, may be achieved through careful choice of spectator ligand scaffolds. However, the challenge of controlling such undesirable phosphine coordination chemistry points also to the exciting prospect of exploring a wider range of secondary phosphine substrates than has been exploited previously in catalytic hydrophosphination, for example the less nucleophilic diaminophosphines and phosphonites.

Finally, the outer-sphere, electrophilic catalysis proposed here relies on facile intramolecular hydride transfer directly from Mo-coordinated secondary phosphine to the intermediate phosphacarbocation. However, we note that "quenching" of intermediate phosphacarbanions in established nucleophilic

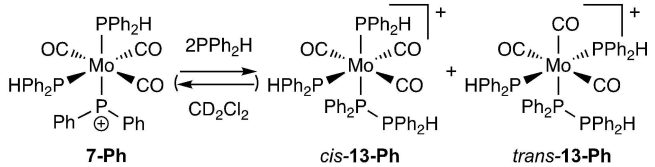

7-Ph *cis*-**13-Ph** *trans*-**13-Ph**

Scheme 13. Possible products of the reaction of **7-Ph** with two equiv. PPh_2H. The cis and trans labels refer to the relative placement of the PPh_2H ligands.

hydrophosphination catalyst systems can also occur through indirect proton transfer from the phosphine substrate, via external base or internal basic sites in the secondary coordination sphere.[1p,7a] By analogy, this suggests an even broader scope for hydride "shuttling" in electrophilic hydrophosphination than we have proposed, and intriguing possibilities for the design of such catalytic systems.

Experimental Section

General experimental details, all NMR spectra, details of full NMR characterization of representative complexes, kinetic data, and Cartesian coordinates of selected computed structures are provided in the Supporting Information.

General procedure for the addition of unsaturated substrates to $[Mo(CO)_4(PR_2H)(PR_2)]^+$ Stoichiometric amounts (0.015–0.034 mmol, 1 equiv) of selected unsaturated substrates were added to complexes **1-R** (0.015–0.034 mmol) in CD_2Cl_2 (500–600 μL). The reactions were monitored by ^{1}H and $^{31}P\{^1H\}$ NMR. Ethylene (~1 atm) was added to a J Young tube containing **1-R** dissolved in CD_2Cl_2 (solution had been degassed by three freeze-pump-thaw cycles) via a Schlenk line. The initial ^{1}H NMR spectra showed approximately 1–1.3 equivalents of ethylene dissolved in solution.

Synthesis of *fac*-$Mo(CO)_3(PTol^p{}_2H)_3$ (6-Tol^p) A Schlenk flask containing *fac*-$Mo(CO)_3(NCCH_3)_3$ (1.0 g, 3.3 mmol) and $P(Tol^p)_2H$ (2.12 g, 10 mmol, 3 equiv) in acetonitrile (20 mL) was stirred for 24 h at room temperature. At this point a white solid had precipitated from the yellow solution, which was filtered, washed with acetonitrile (3×5 mL), and dried under vacuum. Yield: 1.641 g (60 %) white powder. Melting point: 172–174 °C. **$^{31}P\{^1H\}$ NMR** (122 MHz, $CDCl_3$) δ 21.64. **^{1}H NMR** (300 MHz, $CDCl_3$) δ 7.22–7.04 (m, 12H, Tol^p H_o), 6.97–6.87 (m, 12H, Tol^p H_m), 5.43 (d, J = 314.7 Hz, 3H, P–H), 2.19 (s, 18H, *p*-CH_3). **$^{13}C\{^1H\}$ NMR** (126 MHz, $CDCl_3$) δ 220.0 (s, CO), 139.1 (s, C_p), 132.8 (dd, J = 7, 4 Hz, C_o), 131.6 (m, C_i), 129.3 (d, J = 6 Hz, C_m), 21.4 (s, *p*-CH_3). IR (KBr, cm^{-1}): 1941 (ν_{PH}), 1852 (ν_{CO}), 1839 (ν_{CO}). HRMS: 825.17117 (M + H, calc'd 825.17084). Elemental anal. Found (calc'd for $C_{45}H_{45}MoO_3P_3$): C, 65.52 (65.70); H, 5.58 (5.51).

Complex **6-Ph** is a known compound. It was prepared according to the above procedure. Spectroscopic data matches literature data.[33]

General procedure for the synthesis of $[Mo(CO)_3(PR_2H)_2(PR_2)]^+$ (7-R) (Illustrated for the synthesis of **7-Ph**) Complex **6-Ph** (0.256 g, 0.346 mmol) was dissolved in dichloromethane (~10 mL) in a Schlenk flask. To this colourless solution, $[Ph_3C][B(m\text{-}C_6H_3Cl_2)_4]$ (0.292 g, 0.400 mmol, 1.05 equiv) was added with stirring. As the trityl reagent dissolved the solution became deep orange, then changed to a deep green colour over several minutes. Complete conversion to phosphenium complex **7-Ph** took 30 min, as determined by $^{31}P\{^1H\}$ NMR. The stir bar was removed from the solution, which was layered with pentane (~30 mL) and allowed to stand overnight. This gave the product as a viscous green oil. The supernatant was decanted and the residual oil was dried under vacuum. The resulting green powder was washed with pentane (3×5 mL) to remove any remaining Ph_3CH and further dried under vacuum. Yield: 0.400 g (87 %). Melting point: 80–87 °C (decomp). **$^{31}P\{^1H\}$ NMR** (202 MHz, $CDCl_3$) δ 395.6 (dd, J = 84, 46 Hz, $\underline{P}Ph_2^+$), 7.0 (dd, J = 46, 30 Hz, *cis*-$\underline{P}Ph_2H$), 4.1 (dd, J = 84, 30 Hz, *trans*-$\underline{P}Ph_2H$). **^{1}H NMR** (500 MHz, $CDCl_3$) δ 7.68 (t, J = 7.5 Hz, 2H, H_p), 7.60–7.20 (overlapping, 28H, H_{aryl}, PR_2^+ and PPh_2H), 7.06 (m, J = 2.1 Hz, 8H, H_o, $[B(m\text{-}C_6H_3Cl_2)_4]^-$), 6.91 (t, J = 2.1 Hz, 4H, H_p, $[B(m\text{-}C_6H_3Cl_2)_4]^-$), 6.43 (dd, J = 350, 9.6 Hz, P–H, *trans*-PPh_2H), 6.59 (dd, J = 350, 10.6 Hz, P–H, *cis*-PPh_2H). **$^{13}C\{^1H\}$ NMR** (125 MHz, $CDCl_3$): δ 212.8 (two CO, cis to all P-ligands), 207.4 (CO, trans to one PPh_2H), 165.1 (q, J = 50 Hz, C_i, $[B(m\text{-}C_6H_3Cl_2)_4]^-$), 147.8 (s, C_i), 134.3 (s, C_o), 133.4 (s, C_o, $[B(m\text{-}C_6H_3Cl_2)_4]^-$), 132.9 (q, J = 4 Hz, C_m, $[B(m\text{-}C_6H_3Cl_2)_4]^-$), 132.4 cd, J = 11 Hz, C_o), 132.3 (d, J = 11 Hz, C_o), 132.0 (d, J = 2 Hz, C_{aryl}), 131.8 (d, J = 2 Hz, C_{aryl}), 130.0 (d, J = 10 Hz, C_{aryl}), 129.8 (d, J = 10 Hz), 129.4 (d, J = 43 Hz, C_i), 129.3 (d, J = 43 Hz, C_i), 127.6 (J = 43 Hz, C_i) 127.5 (d J = 43 Hz, C_i), 123.2 (s, C_p, $[B(m\text{-}C_6H_3Cl_2)_4]^{<M\text{-}s}$). IR (KBr, cm^{-1}): 2090 (ν_{PH}), 2087 (ν_{PH}), 1990 (ν_{CO}), 1985 (ν_{CO}). HRMS (*m/z*): Positive mode 739.06172 (calc'd 739.06184), negative mode 594.84817 (calc'd 594.84868). Elemental anal. Found (calc'd for $C_{63}H_{44}BCl_8MoO_3P_3$): C, 56.79 (56.43); H, 3.33 (3.37).

For **7-Tol^p**: Yield: 0.767 g, 88 %. Melting point: 80–87 °C (decomp). **$^{31}P\{^1H\}$ NMR** (202 MHz, $CDCl_3$) δ 394.1 (dd, J = 87, 46 Hz, $\underline{P}(Tol^p)_2^+$), 5.7 (dd, J = 44, 30 Hz, *cis*-$\underline{P}Tol^p{}_2H$), 3.0 (dd, J = 83, 30 Hz, *trans*-$\underline{P}Tol^p{}_2H$). **^{1}H NMR** (500 MHz, $CDCl_3$) δ 7.3–7.2 (m, 16H, H_o,H_m, Tol^p), 7.2–7.1 (m, 9H, H_o, H_m, Tol^p), 7.06 (m, J = 2.1 Hz, 8H, H_o, $[B(m\text{-}C_6H_3Cl_2)_4]^-$), 6.91 (t, J = 2.1 Hz, 4H, H_p, $[B(m\text{-}C_6H_3Cl_2)_4]^-$), 6.51 (dd, J = 349, 11.0 Hz, 1H, P–H, *trans*-$PTol^p{}_2H$), 6.35 (dd, J = 347, 9.5 Hz, 1H, P–H, *cis*-$PTol^p{}_2H$), 2.38 (d, J = 11 Hz, 12H, *p*-CH_3, $PTol^p{}_2H$), 2.34 (s, 6H *p*-CH_3, $PTol^p{}_2^+$). **$^{13}C\{^1H\}$ NMR** (126 MHz, $CDCl_3$) δ 209.3 (two CO, cis to all P-ligands), 207.9 (CO trans to one $P(Tol^p)_2H$), 165.1 (q, J = 50 Hz, C_i, $[B(m\text{-}C_6H_3Cl_2)_4]^-$), 145.9 (s, C_p, $PTol^p{}_2^+$), 145.7 dd, J = 48, 4 Hz, C_i, $PTol^p{}_2^+$), 142.6 (s, C_p, *trans*-$PTol^p{}_2H$), 142.4 (s, C_p, *cis*-$PTol^p{}_2H$), 133.5 (s, C_o, $[B(m\text{-}C_6H_3Cl_2)_4]^-$), 132.9 (q, J = 4 Hz, C_m, $[B(m\text{-}C_6H_3Cl_2)_4]^-$), 132.6 (d, J = 5 Hz, C_o, $PTol^p{}_2^+$), 132.4 (d, J = 8 Hz, C_o, $PTol^p{}_2H$), 132.3 (d, J = 8 Hz, C_o, $PTol^p{}_2H$), 130.6 (d, J = 11 Hz, C_m, $PTol^p{}_2H$), 130.4 (d, J = 11 Hz, C_m, $PTol^p{}_2H$), 129.9 (s, C_m, $PTol^p{}_2^+$), 126.3 (d, J = 44 Hz, C_i, $PTol^p{}_2H$), 124.8 (d, J = 44 Hz, C_i, $PTol^p{}_2H$), 123.2 (s, C_p, $[B(m\text{-}C_6H_3Cl_2)_4]^-$), 22.2 (s, *p*-$CH_3$, $PTol^p{}_2^+$), 21.6 (s, *p*-CH_3, *trans*-$PTol^p{}_2H$), 21.5 (s, *p*-CH_3, *cis*-$PTol^p{}_2H$). IR (KBr, cm^{-1}): 2039 (ν_{PH}), 1980 (ν_{CO}), 1939 (ν_{CO}). HRMS: Positive mode 823.15557 (calc'd 823.15574), negative mode 594.84829 (calc'd 594.84868). Elemental anal. Found (calc'd for $C_{69}H_{56}BCl_8MoO_3P_3$): C, 58.00 (58.51); H, 3.94 (3.99).

Gutmann-Beckett experiments to determine Lewis acidity of 7-R General procedure: A 0.017 M stock solution of $Et_3P{=}O$ (0.011 g, 0.082 mmol) in CH_2Cl_2 was prepared in a 5.00 mL volumetric flask. A 0.5 mL aliquot of this mixture was used to dissolve 0.025 mmol of each complex, to give a 3:1 mixture of **7-R**:$Et_3P{=}O$, which was transferred to a J Young NMR tube for analysis by $^{31}P\{^1H\}$ NMR. This method, employing an excess of **7-R**, was used to avoid signal broadening that we observed for the **7-R**:$Et_3P{=}O$ adduct in a 1:1 mixture, which presumably arises from exchange between free and complexed $Et_3P{=}O$. These 3:1 mixtures also contain some minor, unidentified by-products, and a small amount of $Mo(CO)_3(PR_2H)_3$ (**6-R**). Assignment of the $^{31}P\{^1H\}$ signals due to the Gutmann-Beckett adducts was confirmed by $^1H/^{31}P$ HMBC, which showed their correlation with the $Et_3P{=}O$ alkyl signals.

General procedure for the addition of unsaturated substrates to $[Mo(CO)_3(PR_2H)_2(PR_2)]^+$ (7-R) Stoichiometric amounts (0.030–0.060 mmol, 2 equiv) of selected unsaturated substrates were added to complexes **7-R** (0.015–0.030 mmol) in $CDCl_3$ (500-600 μL). The reactions were monitored by ^{1}H and $^{31}P\{^1H\}$ NMR. Ethylene (~1 atm) was added to a J Young tube containing **7-R** dissolved in CD_2Cl_2 (solution had been degassed by three freeze-pump-thaw cycles) via a Schlenk line. Approximately 10 equiv. of ethylene was dissolved in solution for the reaction of **7-Ph**, based on integration of the initial ^{1}H spectrum. This gave complete conversion to **9-Ph-c** within 1 d. For **7-Tol^p**, approximately one equivalent of ethylene was added. This gave a mixture of **8-Tol^p**, some unreacted **7-Tol^p**, and a small amount of **9-Tol^p**, also within 1 d.

Computational details All quantum chemical calculations were carried out with the ORCA 5 program.[37] Geometry optimisations were performed with the PBE functional[38] and the D4 dispersion corrections.[39] The zero-order regular approximation (ZORA) Hamiltonian was used in the one-center approximation to account for

scalar relativistic effects.[40] All-electron ZORA-adapted TZVP basis sets[41] were used for all atoms except for molybdenum, for which the recently developed all-electron SARC-ZORA-TZVP basis set was used.[42] The resolution of the identity (RI) approximation[43] was used for the calculation of Coulomb integrals, in combination with appropriate SARC/J auxiliary basis sets. The effect of solvent (dichloromethane) was tested in an additional series of calculations using the conductor-like polarisable continuum model (CPCM).[44] Transition states were located with the climbing-image nudged elastic band method[45] in the automated two-step zoom procedure implemented in ORCA. Vibrational frequencies were computed analytically in the harmonic approximation to confirm the nature of all stationary points and to compute thermodynamic quantities.

Supporting Information

The authors have cited additional references within the Supporting Information (Ref. [46–48]).

Acknowledgements

We thank NSERC of Canada for funding (Discovery Grant to LR, PGS–D to RB). DAP gratefully acknowledges support by the Max Planck Society.

Conflict of Interests

The authors declare no conflict of interest.

Data Availability Statement

The data that support the findings of this study are available in the supplementary material of this article.

Keywords: electrophilic addition · hydrophosphination · P–H activation · phosphenium complexes · umpolung

[1] Reviews discussing metal-catalyzed hydrophosphination: a) B. T. Novas, R. Waterman, *ChemCatChem* **2022**, *14*, e202200988; b) X. T. Liu, Y. Wu, Q. W. Zhang, *Synlett* **2022**, *33*, 301–306; c) S. Lau, T. M. Hood, R. L. Webster, *ACS Catal.* **2022**, *12*, 10939–10949; d) J. W. K. Seah, R. H. X. Teo, P. H. Leung, *Dalton Trans.* **2021**, *50*, 16909–16915; e) D. Wei, C. Darcel, *J. Org. Chem.* **2020**, *85*, 14298–14306; f) Y. Sarazin, J. F. Carpentier, in *Early Main Group Metal Catalysis: Concepts and Reactions* (Ed.: S. Harder), Wiley, Hoboken, NJ, **2020**, pp. 93–121; g) D. S. Glueck, *J. Org. Chem.* **2020**, *85*, 14276–14285; h) J. K. Liu, J. F. Gong, M. P. Song, *Org. Biomol. Chem.* **2019**, *17*, 6069–6098; i) S. Bezzenine-Lafollee, R. Gil, D. Prim, J. Hannedouche, *Molecules* **2017**, *22*, 1901; j) A. A. Trifonov, I. V. Basalov, A. A. Kissel, *Dalton Trans.* **2016**, *45*, 19172–19193; k) S. A. Pullarkat, *Synthesis* **2016**, *48*, 493–503; l) C. A. Bange, R. Waterman, *Chem. Eur. J.* **2016**, *22*, 12598–12605; m) V. Rodriguez-Ruiz, R. Carlino, S. Bezzenine-Lafollee, R. Gil, D. Prim, E. Schulz, J. Hannedouche, *Dalton Trans.* **2015**, *44*, 12029–12059; n) M. D. Greenhalgh, A. S. Jones, S. P. Thomas, *ChemCatChem* **2015**, *7*, 190–222; o) V. Koshti, S. Gaikwad, S. H. Chikkali, *Coord. Chem. Rev.* **2014**, *265*, 52–73; p) L. Rosenberg, *ACS Catal.* **2013**, *3*, 2845–2855; q) S. A. Pullarkat, P. H. Leung, *Top. Organomet. Chem.* **2013**, *43*, 145–166.
[2] See reference 1p and references therein.
[3] For discrete examples of alkene insertion into M-PR_2 bonds, see K. M. E. Burton, D. A. Pantazis, R. G. Belli, R. McDonald, L. Rosenberg, *Organometallics* **2016**, *35*, 3970–3980, and references therein.
[4] a) S. G. Dannenberg, D. M. Seth, E. J. Finfer, R. Waterman, *ACS Catal.* **2023**, *13*, 550–562; b) I. V. Lapshin, A. V. Cherkasov, A. F. Asachenko, A. A. Trifonov, *Chem. Commun.* **2020**, *56*, 12913–12916; c) S. G. Dannenberg, R. Waterman, *Chem. Commun.* **2020**, *56*, 14219–14222; d) M. P. Cibuzar, S. G. Dannenberg, R. Waterman, *Isr. J. Chem.* **2020**, *60*, 446–451; e) I. V. Lapshin, O. S. Yurova, I. V. Basalov, V. Y. Rad'kov, E. I. Musina, A. V. Cherkasov, G. K. Fukin, A. A. Karasik, A. A. Trifonov, *Inorg. Chem.* **2018**, *57*, 2942–2952; f) C. A. Bange, M. A. Conger, B. T. Novas, E. R. Young, M. D. Liptak, R. Waterman, *ACS Catal.* **2018**, *8*, 6230–6238; g) M. Espinal-Viguri, A. K. King, J. P. Lowe, M. F. Mahon, R. L. Webster, *ACS Catal.* **2016**, *6*, 7892–7897; h) A. M. Geer, A. L. Serrano, B. de Bruin, M. A. Ciriano, C. Tejel, *Angew. Chem. Int. Ed.* **2015**, *54*, 472–475; i) M. B. Ghebreab, C. A. Bange, R. Waterman, *J. Am. Chem. Soc.* **2014**, *136*, 9240–9243.
[5] a) M. Gediga, S. H. Schlindwein, J. Bender, M. Nieger, D. Gudat, *Angew. Chem. Int. Ed.* **2017**, *56*, 15718–15722; b) C. A. Caputo, M. C. Jennings, H. M. Tuononen, N. D. Jones, *Organometallics* **2009**, *28*, 990–1000.
[6] Mulliken charge distributions calculated for bis(arylamino)phosphenium ligands at $RhCl(PH_3)_2$ and $[Rh(PH_3)_2]^+$ fragments indicate marginal transfer of positive charge from P(phosphenium) to Rh. R. T. Baker, in *Abstracts of Papers of the American Chemical Society, Vol. 227*, **2004**, pp. U1287-U1287.
[7] a) R. G. Belli, J. Yang, E. N. Bahena, R. McDonald, L. Rosenberg, *ACS Catal.* **2022**, *12*, 5247–5262; b) R. G. Belli, K. M. E. Burton, S. A. Rufh, R. McDonald, L. Rosenberg, *Organometallics* **2015**, *34*, 5637–5646.
[8] a) C. M. Feil, T. D. Hettich, K. Beyer, C. Sondermann, S. H. Schlindwein, M. Nieger, D. Gudat, *Inorg. Chem.* **2019**, *58*, 6517–6528; b) D. Gudat, in *Comprehensive Inorganic Chemistry Ii: From Elements to Applications, Vol. 1* (Ed.: J. Reedijk, Poeppelmeier, K.), Elsevier, **2013**, pp. 587–621; c) B. F. Pan, Z. Q. Xu, M. W. Bezpalko, B. M. Foxman, C. M. Thomas, *Inorg. Chem.* **2012**, *51*, 4170–4179; d) H. Nakazawa, *Adv. Organomet. Chem.* **2004**, *50*, 107–143; e) M. B. Abrams, B. L. Scott, R. T. Baker, *Organometallics* **2000**, *19*, 4944–4956; f) D. Gudat, *Coord. Chem. Rev.* **1997**, *163*, 71–106; g) A. H. Cowley, R. A. Kemp, *Chem. Rev.* **1985**, *85*, 367–382.
[9] a) L. K. Oliemuller, C. E. Moore, C. M. Thomas, *Inorg. Chem.* **2023**, *62*, 13997–14009; b) L. K. Oliemuller, C. E. Moore, C. M. Thomas, *Inorg. Chem.* **2022**, *61*, 19440–19451; c) B. Stadelmann, J. Bender, D. Forster, W. Frey, M. Nieger, D. Gudat, *Dalton Trans.* **2015**, *44*, 6023–6031; L. Rosenberg, *Coord. Chem. Rev.* **2012**, *256*, 606–626 (and references therein).
[10] a) H. F. K. Bumraiwha, B. T. Sterenberg, *J. Organomet. Chem.* **2022**, *980–981*, 122511; b) R. C. King, S. Nilewar, B. T. Sterenberg, *J. Organomet. Chem.* **2019**, *880*, 68–74; c) S. NIlewar, A. Jayaraman, B. T. Sterenberg, *Organometallics* **2018**, *37*, 4699–4710; d) A. Jayaraman, S. Nilewar, T. V. Jacob, B. T. Sterenberg, *ACS Omega* **2017**, *2*, 7849–7861; e) A. Jayaraman, B. T. Sterenberg, *Organometallics* **2016**, *35*, 2367–2377.
[11] Free phosphenium triflates, $R_2P^+OTf^-$, generated in situ from the addition of Tf_2O to secondary phosphine oxides, have also been used in a range of stoichiometric electrophilic phosphination reactions involving alkyne cycloaddition and/or aromatic C–H substitution, and free phospheniums (masked as phosphireniums in the presence of internal alkynes) have been shown to act as electrophilic organocatalysts for the hydrosilylation of ketones. a) C. H. Yang, H. H. Fan, H. M. Li, S. Y. Hou, X. K. Sun, D. H. Luo, Y. C. Zhang, Z. T. Yang, J. B. Chang, *Org. Lett.* **2019**, *21*, 9438–9441; b) K. Nishimura, K. Hirano, M. Miura, *Org. Lett.* **2019**, *21*, 1467–1470; c) K. Nishimura, Y. Unoh, K. Hirano, M. Miura, *Chem. Eur. J.* **2018**, *24*, 13089–13092; d) Y. Unoh, K. Hirano, M. Miura, *J. Am. Chem. Soc.* **2017**, *139*, 6106–6109; e) D. Gasperini, S. E. Neale, M. F. Mahon, S. A. Macgregor, R. L. Webster, *ACS Catal.* **2021**, *11*, 5452–5462.
[12] R. G. Belli, D. A. Pantazis, R. McDonald, L. Rosenberg, *Angew. Chem. Int. Ed.* **2021**, *60*, 2379–2384.
[13] a) M. Gediga, C. M. Feil, S. H. Schlindwein, J. Bender, M. Nieger, D. Gudat, *Chem. Eur. J.* **2017**, *23*, 11560–11569; b) S. S. Snow, D. X. Jiang, R. W. Parry, *Inorg. Chem.* **1987**, *26*, 1629–1631.
[14] S. Burck, D. Gudat, M. Nieger, W. W. Du Mont, *J. Am. Chem. Soc.* **2006**, *128*, 3946–3955.
[15] J. J. Zhang, J. D. Yang, J. P. Cheng, *Angew. Chem. Int. Ed.* **2019**, *58*, 5983–5987.
[16] A. W. H. Speed, *Chem. Soc. Rev.* **2020**, *49*, 8335–8353.
[17] R. Dobrovetsky, K. Takeuchi, D. W. Stephan, *Chem. Commun.* **2015**, *51*, 2396–2398.
[18] A $^{31}P\{^1H\}$ shift of ~105 ppm has been reported for the bridging diphenylphosphido ligand in the Mo(0) dimer $[(CO)_4Mo(\mu\text{-}PPh_2)Mo$-

$(CO)_4(PPh_2H)]^-$, while the same ligand in the Mo(I) dimer $[(CO)_4Mo]_2(\mu\text{-}PPh_2)_2$ appears at 233 ppm. S. G. Shyu, M. Calligaris, G. Nardin, A. Wojcicki, *J. Am. Chem. Soc.* **1987**, *109*, 3617–3625.
[19] a) O. Arias, H. Ehrhorn, J. Hardter, P. G. Jones, M. Tamm, *Organometallics* **2018**, *37*, 4784–4800; b) M. A. Alvarez, A. Inmaculada, M. E. Garcia, D. Garcia-Vivo, M. A. Ruiz, J. Suárez, *Organometallics* **2012**, *31*, 2749–2763.
[20] V. Varela-Izquierdo, A. M. Geer, J. Navarro, J. A. Lopez, M. A. Ciriano, C. Tejel, *J. Am. Chem. Soc.* **2021**, *143*, 349–358.
[21] $^{31}P\{^1H\}$ signals due to trace amounts of several unidentified products are observed at 4–15 ppm for mixtures of **1**-**R** with methylacrylate at times $\geq$ 4 h.
[22] V. Muir, MSc thesis, University of Victoria (Canada), **2023**.
[23] An alternative mechanism could involve isomerization as a first step, followed by electrophilic addition and hydride transfer. This leaves open the possibility that the addition and H^- transfer steps could be occurring in a concerted fashion.
[24] H. Mayr, G. Lang, A. R. Ofial, *J. Am. Chem. Soc.* **2002**, *124*, 4076–4083.
[25] Faster hydride transfer can circumvent the γ-deprotonation of alkyl-substituted phosphacarbocations in this stoichiometric mechanism (see reactivity of **7**-**R**) but such deprotonation chemistry may pose challenges under catalytic conditions, where excess phosphine can act as an external base. This could be addressed through careful choice of unsaturated substrate, but ultimately represents a further catalyst design challenge (see Conclusions).
[26] Monitoring of the addition of trityl cation to **1**-**Ph** over 3 d shows very slow production of $HCPh_3$, with concurrent loss of the $^{31}P\{^1H\}$ phosphenium signal and the ^1H P–H signal for **1**-**Ph** (see Supporting Information). However, no new phosphenium signal due to the putative bis(phosphenium) dication appears.
[27] P. Erdmann, L. Greb, *Angew. Chem. Int. Ed.* **2022**, *61*, e202114550.
[28] I. B. Sivaev, V. I. Bregadze, *Coord. Chem. Rev.* **2014**, *270*, 75–88.
[29] For example, $^{31}P\{^1H\}$ NMR of *trans*-**9**-**Ph**-**a**, which results from the addition of 1,1-diphenylethylene to **7**-**Ph**, shows a triplet at 380.8 ppm due to the phosphenium ligand and a doublet at 33.8 due to the hydrophosphination products, with $^2J_{PP} = 43$ Hz. See Tables S1-3 for ^{31}P NMR data for all "clean" hydrophosphination reactions.
[30] Cationic polymerization of ethyl vinyl ether is known. U. Eismann, S. Spange, *Macromolecules* **1997**, *30*, 3439–3446.
[31] Reactions showing incomplete conversion to **9**-**R** may also reflect further diminished phosphenium electrophilicity in **8**-**R**, in which one PR_2H ligand has been replaced with a more electron-rich tertiary product phosphine **P**. However, these conversions and product distributions are probably affected also by steric congestion due to the presence of an additional phosphine ligand in these bis(phosphine) phosphenium complexes.
[32] a) H. Mayr, T. Bug, M. F. Gotta, N. Hering, B. Irrgang, B. Janker, B. Kempf, R. Loos, A. R. Ofial, G. Remennikov, H. Schimmel, *J. Am. Chem. Soc.* **2001**, *123*, 9500–9512; b) https://www.cup.uni-muenchen.de/oc/mayr/DBintro.html (accessed October 31, 2023); c) http://www.cup.lmu.de/oc/mayr/MayrPoster.html (accessed October 31, 2023).
[33] $PPh_2CH_2CHPh_2$ appears as a singlet at −20.5 ppm, and $PPh_2CH_2CH_2Ph$ appears as a singlet at −15.9 ppm (C_6D_6). B. Freitag, P. Stegner, K. Thum, C. A. Fischer, S. Harder, *Eur. J. Inorg. Chem.* **2018**, *2018*, 1938–1944.
[34] $^{31}P\{^1H\}$ shifts for free $[Ph_2P\text{–}PPh_2H]^+$ vary with solvent and counterion, with PPh_2H appearing at 3 to 4.5 ppm and PPh_2 at −25.4 to −28.4 ppm. A $^1J_{PP}$ value of 320 Hz observed at low concentrations of the ion is not resolved at higher concentrations. See reference 17 and: G. Pearce, A. M. Borys, E. R. Clark, H. J. Shepherd, *Inorg. Chem.* **2018**, *57*, 11530–11536.
[35] H. Kim, Z. Qu, S. Grimme, N. Al-Zuhaika, D. W. Stephan, *Angew. Chem. Int. Ed.* **2023**, *62*, e202312587, and references therein.
[36] P. B. Glaser, T. D. Tilley, *J. Am. Chem. Soc.* **2003**, *125*, 13640–13641.
[37] a) F. Neese, F. Wennmohs, U. Becker, C. Riplinger, *J. Chem. Phys.* **2020**, *152*, 224108; b) F. Neese, *WIREs Comput. Mol. Sci.* **2022**, *12*, e1606.
[38] J. P. Perdew, K. Burke, M. Ernzerhof, *Phys. Rev. Lett.* **1996**, *77*, 3865–3868.
[39] E. Caldeweyher, C. Bannwarth, S. Grimme, *J. Chem. Phys.* **2017**, *147*, 034112.
[40] a) E. van Lenthe, E. J. Baerends, J. G. Snijders, *J. Chem. Phys.* **1993**, *99*, 4597–4610; b) R. van Leeuwen, E. van Lenthe, E. J. Baerends, J. G. Snijders, *J. Chem. Phys.* **1994**, *101*, 1272–1281; c) E. van Lenthe, E. J. Baerends, J. G. Snijders, *J. Chem. Phys.* **1994**, *101*, 9783–9792.
[41] a) D. A. Pantazis, X. Y. Chen, C. R. Landis, F. Neese, *J. Chem. Theory Comput.* **2008**, *4*, 908–919; b) A. Schäfer, C. Huber, R. Ahlrichs, *J. Chem. Phys.* **1994**, *100*, 5829–5835; c) D. A. Pantazis, F. Neese, *WIREs Comput. Mol. Sci.* **2014**, *4*, 363–374.
[42] J. D. Rolfes, F. Neese, D. A. Pantazis, *J. Comput. Chem.* **2020**, *41*, 1842–1849.
[43] a) M. Sierka, A. Hogekamp, R. Ahlrichs, *J. Chem. Phys.* **2003**, *118*, 9136–9148; b) R. A. Kendall, H. A. Früchtl, *Theor. Chem. Acc.* **1997**, *97*, 158–163.
[44] M. Cossi, N. Rega, G. Scalmani, V. Barone, *J. Comput. Chem.* **2003**, *24*, 669–681.
[45] G. Henkelman, B. P. Uberuaga, H. Jónsson, *J. Chem. Phys.* **2000**, *113*, 9901–9904.
[46] T. Campbell, A. M. Gibson, R. Hart, S. D. Orchard, S. J. A. Pope, G. Reid, *J. Organomet. Chem.* **1999**, *592*, 296–305.
[47] F. Edelmann, P. Behrens, S. Behrens, U. Behrens, *J. Organomet. Chem.* **1986**, *310*, 333–355.
[48] D. J. Darensbourg, R. L. Kump, *Inorg. Chem.* **1978**, *17*, 2680–2682.

Manuscript received: September 8, 2023
Accepted manuscript online: January 19, 2024
Version of record online: February 1, 2024